

# Self-optimizing Visual Servoing Control for Microassembly Robotic Depth Motion

Min Wang, Xiadong Lv, Xinhuan Huang

Department of Control Science and Engineering, Huazhong University of Science and Technology  
Wuhan 430074, China  
wm526@163.com

**Abstract** - This paper presents a self-optimizing visual servoing control method for microassembly robotic depth motion. To measure micromanipulator depth motion, a normalized gray-variance focus measure operator is developed using depth from focus techniques. The extracted defocus features are theoretically distributed with one peak point which can be applied to locate the microscopic focal depth via self-optimizing control. Tracking differentiators are developed to suppress noises and track the features and their differential values without oscillation. Based on the differential defocus signals a coarse-to-fine self-optimizing controller is presented for micromanipulator to precisely locate focus depth. Experimental results of microassembly robotic depth motion demonstrate the performance of the proposed method with depth servo error of 7.5 $\mu$ m.

**Index Terms** – *Microscopic visual servoing, depth from focus, tracking differentiator, self optimization control*.

## I. INTRODUCTION

Image-based microscopic visual servoing is now the key technique in microassembly robot system. Micromanipulator depth motion control presents a great challenge to microscopic visual servoing due to the limited depth of field in microscopic vision. Considering the requirements of measurement precision and micro-space configuration, some common depth detection methods, such as macro stereo vision, laser, ultrasonic, can hardly be used in microscopic image depth computation. The algorithm of depth from defocus (DFD) directly extracts depth information from monocular defocus images and therefore receives a lot of attention in recent years. Pentland firstly proposed the Gaussian model of point spread function (PSF) in optical defocus imaging [1]. Then he employed inverse filtering method to estimate depth by focus and defocus images with different camera parameters. Later many researchers focused on the Pentland's model to improve the DFD algorithm, such as [2-3]. As a kind of passive computer vision method, the DFD algorithm has an advantage of indirect measurement on object's depth with fewer demands on geometrical space configuration. However, the method mostly depends on a precise calibration to camera's PSF model and its high computation costs can hardly meet the requirements of micromanipulator's real-time visual servoing along image depth way.

Depth from focus (DFF) is another important technique in computer vision, which has been widely used in many

microscopic auto-focusing systems. Compared with DFD algorithm, DFF method with low computation costs does not need prior knowledge to camera imaging model. In DFF algorithm focus measure operators (FMO) has been investigated to compute global defocus features from depth images [4-5]. The extracted defocus feature curve should be theoretically distributed with only one peak and represents the depth position of microscopic focal plane. Accordingly micromanipulator can automatically locate the microscopic focal position by searching the peak point with minimum differential values of defocus features. This is the so-called self-optimizing control problem regarded by vision-based microassembly depth motion servoing. The extracted defocus features from depth images usually include lots of random noises which may severely reduce the control performance of depth vision controller. Tracking differentiator (TD) has been proved to be an effective way to suppress noises and extract differential signals from dirty sampling [6]. It can smoothly track input variables and their differential values with less oscillation. Compared with some common differential methods, TD can greatly improve vision controller's performance under random noise disturbances [7].

To describe micromanipulator depth motion we adopt a normalized gray-variance FMO to compute defocus image features. Nonlinear tracking differentiators are employed to track the features and their differential values smoothly. Based on the tracked differential features by TD, a coarse-to-fine self-optimizing vision controller is then presented for micromanipulator to precisely locate assembly plane along the microscopic depth way. The paper is organized as: Section II gives a brief description to microscopic imaging model. Focus measure operator and its defocus image features are discussed detailedly in Section III. Section IV introduces the self-optimizing vision control of microassembly depth motion using TD and DFF techniques. Experimental results of microscopic depth visual servo control can be found in Section V. Section VI summarizes the whole paper.

## II. MICROSCOPIC DEFOCUS IMAGING MODEL

Compared with general vision, microscopic vision owns a limited depth of field. It leads to a blur image in microscopic view when object moves beyond microscope's focal range. Defocus image presents difficulties in depth estimation since object can hardly be located in 2D image plane using common geometrical matching technique. Therefore DFD and DFF

methods usually estimate object depth based on the defocus PSF model with blur parameter  $\sigma$ .

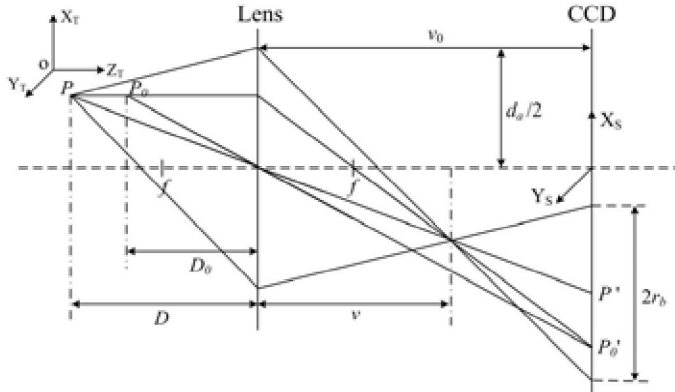


Fig.1 Microscopic defocus image model

Microscopic defocus image model is shown as Fig.1.  $f$  is the focal length of microscope considering thin convex lens. With a fixed microscopic magnification,  $v_0$  is a constant parameter representing the distance between the lens and the imaging plane of CCD camera. According to the well-known thin lens formula,  $f^{-1} = D_0^{-1} + v_0^{-1}$ ,  $D_0$  is the focal depth where object  $P_0$  can obtain a focus imaging  $P_0'$  on the CCD plane. If object point  $P$  with depth  $D$  is not in focus,  $D \neq D_0$ , its imaging on the CCD plane is not a single point but a blur circle with centre point  $P'$  and radius  $r_b$ . According to the Pentland's method, the point spread function of blur circle can be approximated by 2D Gaussian function [1]:

$$h(x, y, \sigma) = \frac{1}{2\pi\sigma^2} \exp \frac{-(x^2 + y^2)}{2\sigma^2} \quad (1)$$

where  $\sigma$  is the so-called blur parameter,  $\sigma = k \cdot r_b$ , and  $k$  is a positive scalar. Considering the geometrical imaging relationship in Fig.1, there exists:

$$\sigma = \frac{kd_a}{2f} (v_0 - f - \frac{Fv_0}{D}) \quad (2)$$

where  $d_a$  represents the aperture diameter of microscope lens. In view of (2), when optical parameters,  $f, v_0, k, d_a$ , are all known, the blur parameter  $\sigma$  can be only determined by the imaging depth  $D$ ,  $\sigma = \sigma(D)$ . Assume there exists one point  $(x, y)$  in blur image, its defocus image intensity  $g(x, y)$  can be calculated through the following convolution:

$$g(x, y) = f(x, y) \otimes h(x, y, \sigma(D)) \quad (3)$$

where  $f(x, y)$  describes the focus intensity of point  $(x, y)$ ,  $h(x, y, \sigma(D))$  is the point's point spread function, and  $\otimes$  represents the convolution operation. In view of (2) and (3), the image depth variable  $D$  can be recovered through inverse filtering based on a well knowledge of PSF model  $h(x, y, \sigma(D))$ .

However, the above discussion is only concerned about one object point and its imaging. Actually, a microscopic image composes of many imaging points and there exists overlap between each point's blur circles. Since depth  $D$  differs at various object points, blur parameter  $\sigma$  would vary

all over the image and the defocus system (3) would be shift-variant. This leads to great difficulties in DFD's depth estimation. To simplify the problem, most DFD algorithms assume the defocus points within one image window  $w$  are distributed with the same depth  $D_w$ , and the corresponding blur parameter  $\sigma_w$  is then a fixed value,  $\sigma_w = \sigma(D_w)$ . Under the assumption the image depth  $D_w$  can be resolved through inverse filtering or other improved DFD techniques.

According to the above introduction, DFD's depth estimation depends on a well knowledge of optical PSF model and camera parameters, and it also needs high time-cost computation during inverse filtering. In some dynamic and unknown cases DFD method can not meet the real-time requirements of micromanipulator depth servoing. Therefore, it may be necessary to develop a fast depth estimation algorithm for microscopic visual servoing.

### III. MICROSCOPIC DEPTH ESTIMATION USING DEPTH FOCUS

Depth from focus method employees focus measure operator to describe defocus intensity in 2D image domain. The output of an ideal FMO, defocus image feature, is defined as having a maximum value at the best focused image/position and decreasing as defocus increases. Based on FMO the focus depth can be estimated through the defocus feature's optimization. DFF techniques have been successfully applied in microscopy autofocusing. A comparison of 18 algorithms used FMO can be found in [8] and they have been classified into four groups: derivative-based algorithms, statistics-based algorithms, histogram-based algorithms and intuitive algorithms.

With low computation costs, the statistics-based DFF algorithms are generally less sensitive to noises than others. So we adopt a normalized gray-variance FMO to extract defocus features from microassembly images. The algorithm firstly computes variations in gray level among image pixels, and then normalizes the final output with the mean intensity to compensate for the differences in average image intensity:

$$F = \frac{1}{m \cdot n \cdot \mu} \sum \sum_{(i,j) \in L} (g(i, j) - \mu)^2 \quad (4)$$

where  $F$  represents the defocus image feature by FMO, and  $L$  is the selected window in defocus image for DFF computation.  $L$  is  $m \times n$  sized with the center point  $(i_0, j_0)$ ,  $L : \{(i, j) : i_0 - m/2 \leq i \leq i_0 + m/2, j_0 - n/2 \leq j \leq j_0 + n/2\}$ .  $g(i, j)$  stands for the gray value of point  $(i, j)$  and  $\mu$  describes the mean intensity of image window  $L$ .

Fig.2 shows a microscopic image sequence of micromanipulator depth motion. With the micromanipulator moving along optical depth axis, we can notice that the imaging defocus of section  $L$  firstly decreases, and then increases after passing the best focused depth position  $D_0$  in Fig.2-(b). Accordingly the normalized gray-variance FMO computes the global feature to describe defocus imaging in  $L$ , and  $F$  should obtain the maximum value  $F_{\max}$  at  $D_0$ .

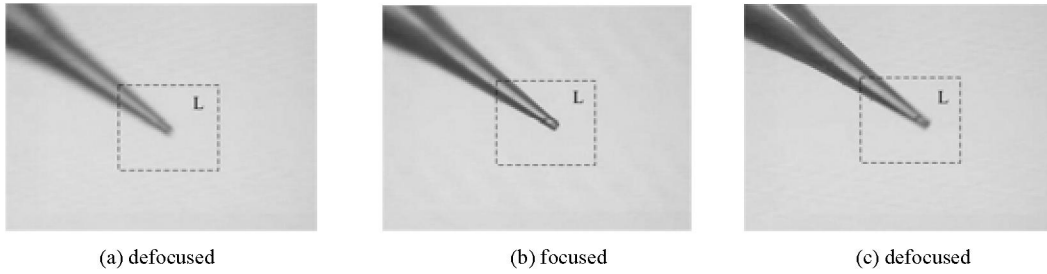


Fig. 2 Microscopic image sequence of micromanipulator depth motion

In term of the above discussion, the ideal defocus image feature curve  $G(D, F)$  should be distributed with only one peak, as shown in Fig.3. The peak point  $(D_0, F_{\max})$  represents the focal depth  $D_0$  with the maximum defocus feature  $F_{\max}$ , and the derivative of  $F$  with respect to  $D$  should get zero,  $\partial F / \partial D|_{D=D_0} = 0$ . As object moves away from  $D_0$ , the image feature decreases with defocus increasing.

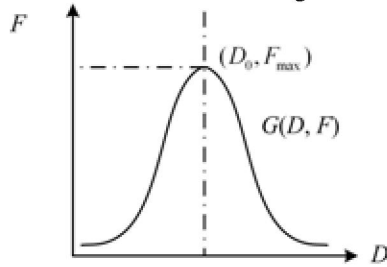


Fig.3 Defocus image feature curve

The peak distribution of DFF feature presents a feasible way for micromanipulator to determine microscopic focal depth. According to the differential values of  $F$  with respect to  $D$ , vision controller can adjust micromanipulator's depth motion to search the peak position with maximum defocus feature. This is a self-optimizing control problem regarded by vision-based microassembly depth motion servo below.

#### IV. SELF-OPTIMIZING VISION CONTROL FOR MICROASSEMBLY DEPTH MOTION

##### A. Self-optimization of defocus image feature

Image-based microscopic visual servoing usually adjusts micromanipulator's motion based on image feature error. Micromanipulator depth motion control is performed with the

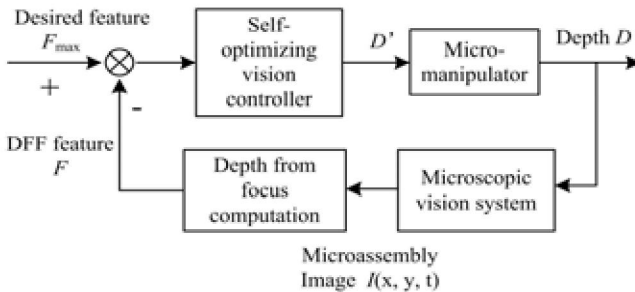


Fig. 4 Self-optimizing control of microassembly depth motion based on defocus image feature

self-optimization of defocus image feature. The depth control aim is to automatically guide manipulator to move toward the focus depth position  $D_0$  with the maximum defocus feature  $F_{\max}$ . Fig. 4 is its control block diagram.

Referring to the peak distribution characteristic of DFF feature, the self-optimizing vision controller adjusts micromanipulator's motion by:

$$D'_{k+1} = \begin{cases} D_k, & \text{if } |dF(D_k)/dD| < \varepsilon \\ D_k + \lambda \cdot \frac{dF(D_k)}{dD}, & \text{else} \end{cases}, \quad \lambda > 0 \quad (5)$$

where  $D_k$  is the manipulator's depth position at the  $k$ -th interval, and  $D'_{k+1}$  represents the controller's output for manipulator motion. Define  $\varepsilon$  as a threshold for the differential value  $dF/dD$ . If  $|dF(D_k)/dD| < \varepsilon$ , we determine that manipulator arrives at the peak depth and then visual servo ends.

According to the above control algorithm, depth motion servo mainly depends on a proper estimation to the differential signals  $dF/dD$ . However the extracted defocus features by DFF usually include lots of random noises and common difference methods may severely recede the performance of the self-optimizing controller under noise disturbances.

##### B. Microassembly depth motion servo using tracking differentiator

Tracking differentiator (TD) has proved to be an effective way to suppress noises and extract differential signals from dirty sampling. It has been widely used to improve control methods with difference computation. As a special nonlinear filter with the input  $v(t)$ , TD owns two output variables,  $x_1(t)$  and  $x_2(t)$ ,  $x_2(t) = \dot{x}_1(t)$ .  $x_1(t)$  tracks  $v(t)$  and  $x_2(t)$  approximates to the general derivative of the input signal  $v(t)$ . The discrete version of TD is written as:

$$\begin{cases} x_1(t+1) = x_1(t) + h \cdot x_2(t) \\ x_2(t+1) = x_2(t) + h \cdot fst(x_1(t) - v(t), x_2(t), r, h_0) \end{cases} \quad (6)$$

where  $h$  represents the integral interval. The nonlinear function  $fst(x_1, x_2, r, h_0)$  is defined as:

$$d = rh_0, d_0 = dh_0, y = x_1 + h_0 x_2; \quad (7)$$

$$a_0 = \sqrt{d^2 + 8r|y|}; \quad (8)$$

$$a = \begin{cases} x_2 + \frac{y}{h_0}, & |y| < d_0 \\ x_2 + \frac{\text{sgn}(y) \cdot (a_0 - d)}{2}, & |y| \geq d_0 \end{cases} \quad (9)$$

$$fst = \begin{cases} -r \cdot \frac{a}{d}, & |a| \leq d \\ -r \cdot \text{sgn}(a), & |a| > d \end{cases} \quad (10)$$

where  $r$  is the tracking parameter. TD tracks the input variable more quickly with larger  $r$ , but it would also induce more high frequency noises;  $h_0$  represents the filtering parameter. Larger  $h_0$  leads to TD tracking more smoothly and more slowly at the same time. So it is necessary to make a compromise between tracking and filtering with the proper parameters  $r$  and  $h_0$ .

To improve the servo precision of microassembly depth motion, a coarse-to-fine control algorithm is developed based on (5):

$$D'_{k+1} = \begin{cases} D_k, & \text{if } |dF/dD| < \varepsilon_1 \\ D_k + \lambda_1 \cdot dF/dD, & \text{if } \varepsilon_1 \leq |dF/dD| \leq \varepsilon_2 \\ D_k + \lambda_2 \cdot dF/dD, & \text{else} \end{cases} \quad (11)$$

where the scalar parameters exist  $\lambda_2 > \lambda_1 > 0$ . According to (11), the controller adopts the coarse adjustment as  $|dF/dD| > \varepsilon_2$ . If  $\varepsilon_1 \leq |dF/dD| \leq \varepsilon_2$ , the fine control will be executed. The depth servo ends when  $|dF/dD| < \varepsilon_1$ .

To obtain a proper estimation of the differential defocus feature,  $dF/dD$  can be re-written as:

$$\frac{dF}{dD} = \frac{dF/dt}{dD/dt} \quad (12)$$

Employee two tracking differentiators to compute the differential signals  $dF/dt$  and  $dD/dt$  respectively. Then substitute (12) into (11) to perform the coarse-to-fine depth motion servoing. The control block diagram is as shown in Fig.5.

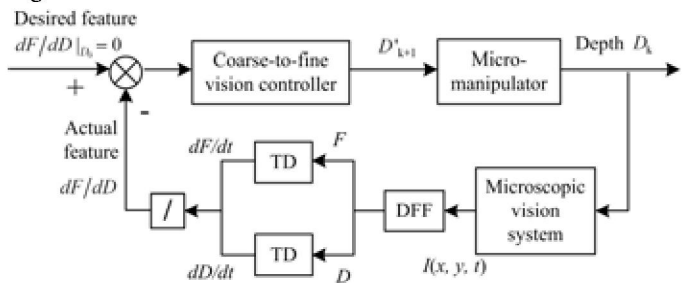


Fig. 5 Microassembly depth visual servoing using tracking differentiator

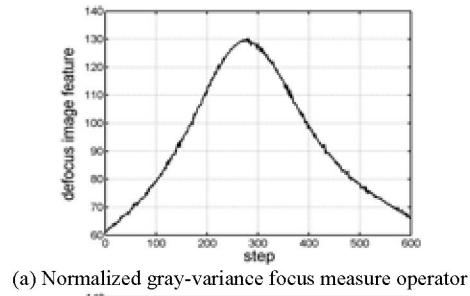
## V. EXPERIMENTAL RESULTS

Microassembly depth servoing experiments were conducted with the microassembly robot system in our lab [9]. The micromanipulator is provided with three translational DOF and one orientation DOF. The translational motion is

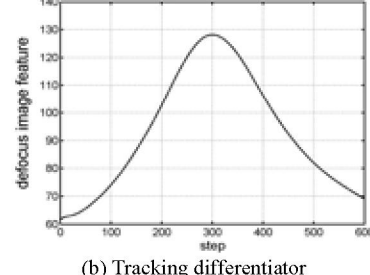
based on a 3 DOF Bayside micropositioning platform with a Cartesian configuration. It has a moving travel of 50mm and a repeatability of 2.5um along each of X, Y and Z axes. The platform is driven by Panasonic AC servo motors with a step resolution 0.25um. The orientation motion is actuated by Faulhaber DC micromotor with a resolution of 0.01°. The above four axes motion control was accomplished utilizing a programmable multi-axis servo motion driver manufactured by Googol Tech. Micromanipulator's motion is monitored by the microscopic vision unit with 2× microscope objective and 400\*300 pixel sized CCD image.

### A. DFF defocus image feature extraction

The micromanipulator performed a continuous motion along the optical depth axis with the moving step 5um and the moving travel 3mm. During the motion, the normalized gray-variance FMO with tracking differentiator was employed to compute the defocus image feature and its differential signal. Experimental results are shown by Fig.6 and Fig.7. Fig.6 (a) is the defocus image feature curve extracted by FMO and it includes random noise disturbances. Fig.6 (b) is the tracked result by TD and it distributes more smoothly compared with the FMO output. Using the common center-difference method its differential defocus feature is described by Fig.7 (a), which has been severely polluted by noises. Fig.7 (b) represents the TD's estimated differential defocus values with great improvement on signal quality.

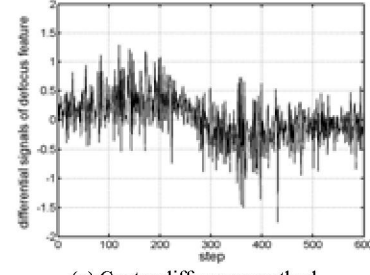


(a) Normalized gray-variance focus measure operator

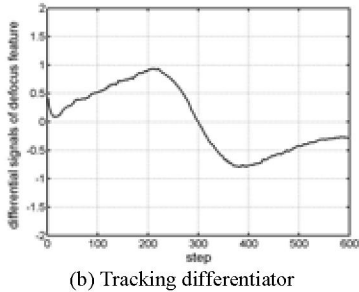


(b) Tracking differentiator

Fig. 6 Defocus feature curve of microassembly depth motion



(a) Centre difference method



(b) Tracking differentiator

Fig. 7 Differential signals of defocus image features

### B. Microassembly depth motion servoing

To compare with the proposed coarse-to-fine depth servo algorithm, the hill-climbing algorithm widely used in digital camera autofocus system [10] was adopted for micromanipulator depth positioning control. Manipulator's motion step was set  $2.5\mu\text{m}$  with the visual servo cycle 0.1s. The desired focus depth position  $D_0$  was  $630\mu\text{m}$ .

Experimental results of two control algorithms are represented in Fig.8. D1 is the motion trajectory of the proposed method based on TD. After 7.8s the depth control ended and the manipulator arrived at  $D=622.5\mu\text{m}$  with the servoing error of  $7.5\mu\text{m}$ . D2 is the positioning result of the hill-climbing algorithm. Due to random noise disturbances, the control failed with oscillations around the local minima of defocus image feature.

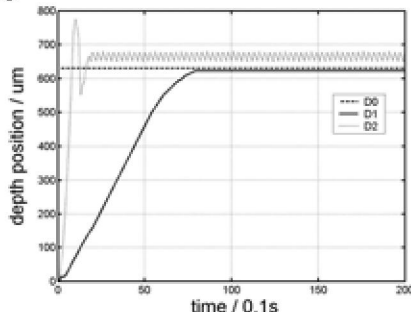


Fig. 8 Microassembly depth positioning experiment by visual servoing

### VI. CONCLUSION

Vision-based microassembly depth motion control presents a great challenge since the limited depth of field of microscopic vision. To measure micromanipulator depth motion, a normalized gray-variance focus measure operator is developed based on depth from focus techniques. The extracted defocus features by DFF are theoretically distributed with one peak point, which can be applied to locate the microscopic focal depth based on self-optimizing control. The estimated defocus features usually include lots of random noises. Nonlinear tracking differentiators are developed to suppress noises and track the features and their differential values without oscillation. Based on the differential defocus signals a coarse-to-fine self-optimizing controller is presented for micromanipulator to precisely locate focus depth by visual servoing. Experimental results of microassembly depth motion demonstrate the performance of the proposed approach with depth servoing error of  $7.5\mu\text{m}$ .

### ACKNOWLEDGMENTS

This work is supported by National Natural Science Foundation of China (No.60275013).

### REFERENCES

- [1] A.P. Pentland. "A new sense for depth of field," *IEEE Trans. Pattern Analysis and Machine Intelligence*, 1987, 9(7): 523-531
- [2] J. Ens, P. Lawrence. "An investigation of methods for determining depth from focus," *IEEE Trans. Pattern Analysis and Machine Intelligence*, 1993, 15(2): 97-107
- [3] D. Ziou, S. Wang, J. Vaillancourt. "Depth from defocus using the hermite transform". Proc. of IEEE Conf. Image Processing. Chicago, pp. 958-962, 1998
- [4] R. A. Jarvis. "Focus optimization criteria for computer image processing," *Microscope*, 1976, 24(2): 163-180
- [5] F. Groen, I. T. Young, G. Lighthart. "A comparison of different focus functions for use in autofocus algorithms," *Cytometry*, 1985, 6(2): 81-91
- [6] J. Han, L. Yuan. "The discrete form of tracking-differentiator," *J. Sys. Sci& Math. Scis*, 1999, 19(3):268-273
- [7] Y.Huang, W. Zhang. "Development of active disturbance rejection controller," *Control Theory and Applications*, 2002, 19(4): 485-492
- [8] Y. Sun, S. Duthaler, B.J. Nelson. "Autofocusing algorithm selection in computer microscopy," Proc. of IEEE/RSJ Int. Conf. Intelligent Robots and Systems, pp. 70-76, 2005
- [9] X. Huang, X. Lv, M. Wang. "Development of a robotic microassembly system with multi-manipulator cooperation," Proc. of IEEE Int. Conf. Mechatronics and Automation, pp. 1197-1201, 2006
- [10]J. Lee. "Implementation of a passive automatic focusing algorithm for digital still camera," *IEEE Trans. on Consumer Electronics*, 1995, 41(3): 449-454